Historic carbon burial spike in an Amazon floodplain lake linked to riparian deforestation near Santarem, Brazil

Luciana M. Sanders[1], Kathryn Taffs[1], Debra Stokes[2], Christian J. Sanders[3], Alex Enrich-Prast[4,5], Leonardo Nogueira Amora[6,7], Humberto Marotta[6,7]

[1]*School of Environment, Science and Engineering, Southern Cross University, Coffs Harbour, New South Wales, Australia.*

[2]*Marine Ecology Research Centre, Southern Cross University, P.O. Box 157, Lismore, NSW 2480, Australia University, P.O. Box 157, Lismore, NSW 2480, Australia*

[3]*National Marine Science Centre, School of Environment, Science and Engineering, Southern Cross University, Coffs Harbour, New South Wales, Australia..*

[4]*Laboratório de Biogeoquímica, Universidade Federal do Rio de Janeiro (UFRJ), Rio d Janeiro (RJ), 21941 971, Brazil.*

[5]*Department of Environmental Change, Linköping University, 581 83, Linköping, Sweden.*

[6]*Ecosystems and Global Change Laboratory (LEMG-UFF) / International Laboratory of Global Change (LINCGlobal). Biomass and Water Management Research Center (NAB-UFF). Graduated Program in Geosciences (Environmental Geochemistry). Universidade Federal Fluminense (UFF), Av. Edmundo March, s/nº – Zip Code: 24210-310, Niteroi/RJ- Brazil.*

[7]*Sedimentary and Environmental Processes Laboratory (LAPSA-UFF). Department of Geography. Graduated Program in Geography. Universidade Federal Fluminense (UFF), Av. Gal. Milton Tavares de Souza, s/nº - Zip Code: 24210-346, Niteroi/RJ- Brazil.*

*Corresponding author. E-mail address; l.sanders.13@student.scu.edu.au

Abstract

Forests along the Amazon Basin produce significant quantities of organic material, a portion of which is deposited in floodplain lakes. Deforestation in the watershed may then have potentially important effects on the carbon fluxes. In this study, a sediment core was extracted from an Amazon floodplain lake to examine the relationship between carbon burial and changing land cover/land use. Historical records from the 1930s and satellite data from the 1970s were used to calculate deforestation rates between 1930 and 1970, and 1970 to 2010 in four zones with different distances from the margins of the lake and its tributaries (100, 500, 1000 and 6000 m buffers). A sediment accumulation rate of ~4 mm $year^{-1}$ for the previous ~120 years was determined from the $^{240+239}Pu$ signatures and the excess ^{210}Pb method. The carbon burial rates ranged between 85 and 298 g C m^{-2} $year^{-1}$, with pulses of high carbon burial in the 1950s, originating from the forest vegetation as indicated by $\delta^{13}C$ and $\delta^{15}N$ signatures. Our results revealed a potentially important spatial dependence of the OC burial in Amazon lacustrine sediments in relation to deforestation rates in the catchment. These deforestation rates were more intense in the riparian vegetation (100 m buffer) during the period 1930 to 1970 and the larger open water areas (500, 1000 and 6000 m buffer) during 1970 to 2010. The continued removal of vegetation from the interior of the forest was not related to the peak of OC burial in the lake, but only the riparian deforestation which peaked during the 1950s. Therefore, this supports the conservation priority of riparian forests as an important management practice for Amazon flooded areas. Our findings suggest the importance of abrupt and temporary events in which some of the biomass released by the deforestation, especially restricted to areas along open water edges, might reach the depositional environments in the floodplain of the Amazon Basin.

1. Introduction

Rivers act as vectors, transporting sediment from land to ocean (Abril et al. 2014). Along this trajectory a significant proportion of the sediment load, including organic material, may be deposited in floodplains, creating zones of carbon accumulation (Smith et al. 2002, Dong et al. 2012, Hoffmann et al. 2013). This process is accelerated during flood events, when rivers and tributaries deposit organic material along the inundated floodplains (Smith et al. 2002). In some climate zones, floodplains are seasonally inundated, with riparian zone vegetation dependent upon this seasonal influx of organic material. The riparian vegetation slows water velocity and traps fine-grained, carbon rich sediments within this low-energy environment (Aalto et al. 2003). Therefore, the riparian vegetation along the floodplains may be important for the organic matter deposition and the Amazon carbon cycle.

The importance of tropical wetland ecosystems in the carbon cycle is well documented (Downing et al. 1993, Melack et al. 2004, Zocatelli et al. 2013, Abril et al. 2014, Marotta et al. 2014). It has been shown that wetlands in the warm tropics are some of the most productive biological communities in the world (Neue et al. 1997), representing an important sink for nutrients (Marotta et al. 2009) and carbon (Peixoto et al. 2016, Sanders et al. 2017), as well as sources of organic substrates to carbon gas production in inland waters (Marotta et al. 2010). However, these wetland ecosystems are also highly threatened by land use activities, especially from deforestation, development of agricultural land and soil degradation (Junk 2013, Lucas et al. 2014).

The Amazon Basin wetlands are being degraded by farming activities such as commercial ranching and an increase in road density (Goulding 1993). Deforestation of

the Amazon Basin commenced ~ 1930 and accelerated toward the end of the 1970's (Skole and Tucker 1993), when an estimated 15% of the pristine rainforest area was lost by the year 2003, increasing to approximately 18% by 2015 (INPE 2016). The ongoing loss of vegetation is responsible for a substantial increase in erosion rates and subsequent sediment inputs into Amazon rivers and lakes (Neill et al. 2013b). Yet these anthropogenic activities are potential sources of allochthonous organic matter that may increase carbon stores in the associated floodplain areas (Diaz and Rosenberg 2008, Stanley et al. 2012).

Jupindá Lake, in the state of Pará, provides an ideal opportunity to investigate historical changes in organic carbon burial in a floodplain lake as a result of the well documented anthropogenic activities within its watershed. This will aid in identifying the little known impacts of land cover changes on recent carbon burial rates in depositional environments of the Amazon floodplain. The objectives of this research are to investigate the effects of deforestation and urban development on carbon burial rates in a tropical floodplain lake. We hypothesize that the historical deforestation in this region of the Amazon may have influenced the OC burial rates in the studied floodplain lake.

2. Methods

The city of Santarem, in central Amazon, was established in the mid-eighteenth century, approximately 650 km upstream from the Amazon River mouth and at its confluence with the Tapajós River (02°25'0.28"S and 54°42'41.57"W, Figure 1). In 1940, Santarém was only a small village, less than 0.5 km^2, surrounded by dense pristine rainforest (estimated from the historical mapping of the Santarém City Hall). This city

quickly expanded, occupying 5.2 km^2 by the end of the 1970s and 49.3 km^2 currently (estimated from satellite images LANDSAT/SRTM). Jupindá Lake is 70 km east of Santarém City, and receives surface water inflow from small streams draining from the forest and the main tributary Curuá-Una River, a large affluent of the Amazon River (Figure 1). The Lake has been affected by the deforestation associated with the expansion of Santarém City. Between the 1940's and 1950's, there was intense deforestation on the margins of rivers and streams in this area, used to supply the markets with wood and forestry products (Amorim 2000, Cruz et al. 2011). In the 1970s, the Curuá-Una River was dammed (Curuá-Una Dam) 45 km upstream of Jupindá Lake to build the first hydroelectric plant of the Amazon Forest (LigockI 2003).

A 60 cm sediment core (diameter 7.5 cm) was collected in 2010 using a gravity corer in the center of the Jupindá Lake (02°27'43.60" S, 54° 5'1.30" W). The sediment core was sub sampled at 2 cm intervals. Dry bulk density (DBD, g cm^{-3}) was determined as the dry sediment weight (g) divided by the initial volume (cm^3). A homogenized portion was acidified (10% HCl following the procedures outlined in Naidu et al. (2000)) to remove carbonate material, then dried and ground to powder for organic carbon (OC), nitrogen (N), $\delta^{13}C$, and $\delta^{15}N$ analyses using a Flash Elemental Analyzer coupled to a Thermo Fisher Delta V IRMS (isotope ratio mass spectrometer). The $\delta^{15}N$ results and the C/N ratios results should be interpreted with caution based on this pre-treatment method (Brodie et al. 2011). Working standards were used (glucose, 10.7 ppt and urea, 41.3 ppt) to calibrate for $\delta^{13}C$. A pair of standards was measured with every 20 samples. These standards were calibrated initially against international absolute standards LSVEC and NIST8542. Analytical precision: C = 0.1 %, N = 0.1%, $\delta^{13}C$ = 0.1‰ and $\delta^{15}N$ = 0.15 ‰.

Samples were prepared for Pu dating following the method of Ketterer et al. (2004) with modifications to enable larger sample mass to be processed as a result of the likely lower Pu concentrations in the Southern Hemisphere (Sanders et al. 2016). To obtain a larger mass, sediment intervals were joined and homogenized so the sediment intervals for the $^{240+239}$Pu dating was 4 cm intervals. Sample aliquots ranging from 14 to 29 grams were dry-ashed at 600 ^{O}C for 16 hours, and leached with 50 mL of 16 M HNO_3. The leaching was conducted overnight at 80^{O}C with added ^{242}Pu yield tracer (NIST 4334g, 19 picograms). Acid leaching (as opposed to complete dissolution with HF) is known to solubilize stratospheric fallout Pu, and there is little possibility that "refractory" HNO_3-insoluble Pu exists in the South America (Sanders et al. 2014). The leachates were diluted to 100 mL, filtered to remove solids, and the aqueous solutions were processed with TEVA resin (EIChrom, Lisle, Il, USA) in order to chemically isolate 3.0 mL Pu fractions in aqueous ammonium oxalate solution suitable for measurements by sector ICPMS. Pu determinations were performed using a VG Axiom MC operating in the single collector (electron multiplier) mode. The system was used with an APEX HF desolvating micronebulizer system (ESI Scientific, Omaha, NE, USA) with an uptake rate of 0.4 mL/minute. Qualitative mass spectral scans (averages of 50 sweeps over the mass range 237.4 – 242.6) were collected for selected samples prior to the electrostatic sector quantitative scanning of ^{238}U+, ^{239}Pu+, ^{240}Pu+, and ^{242}Pu+. Detection limits were evaluated based upon the analysis of two blanks and considerations regarding the obtained mass spectra. A detection limit of 0.01 Bq/kg of $^{239+240}$Pu is applicable for samples of nominal 25 g mass.

For ^{210}Pb dating, an intrinsic germanium detector coupled to a multi-channel analyzer was used. Freeze dried and ground sediments were packed and sealed in gamma tubes. Lead-210 and ^{226}Ra activities were calculated by multiplying the counts per minute by a factor that includes the gamma-ray intensity and detector efficiency determined from standard calibrations. Identical geometry was used for all samples. Lead-210 activities were determined by the direct measurement of the 46.5 KeV gamma peak. Radium-226 activity was determined via the ^{214}Pb daughter at 351.9 KeV. For ^{226}Ra measurements, the packed samples were set aside for at least 21 days to allow for ^{222}Rn to ingrow and establish secular equilibrium between ^{226}Ra and its granddaughter ^{214}Pb. Excess ^{210}Pb activity was calculated by subtracting the supported ^{210}Pb (i.e., ^{226}Ra activity) from the total ^{210}Pb activity. The sediment accretion rate for the previous 120 years was estimated by two methods derived from ^{210}Pb dating, the Constant Initial Concentration (CIC) model assuming that this rate has not varied during the encompassed time span (Appleby and Oldfield 1992), and the Constant Rate of Supply (CRS) model based on a constant influx of unsupported, atmospheric ^{210}Pb that allows a variable sediment rate (Ivanovich and Harmon 1992). Organic carbon accumulation rates were estimated from an average between these the two dating methods ($^{239+240}$Pu and $^{210}Pb_{ex}$), the dry bulk density (g cm^3) and carbon content for each interval of the entire sediment core.

The land use and land cover analysis was based on documented historical information before 1975 and satellite images (Landsat/SRTM, Table 1) from 1975, 1985, 1995 and 2008 available from the United States Geological Survey (USGS). No significant deforestation occurred in the catchment area of the Jupindá Lake until the early 1940's (Amorim 2000, Cruz et al. 2011). Subsequent land/use changes were determined using

satellite images (Gordon 1980, Munyati 2000). All satellite images were from low-water seasons to remove the influence of the flood pulse on the exposed area over years. The resolution of the images was 30 m, except that from the 1970's, which was resampled from 90 to 30 m (Table 1). This approach allowed an assessment of changes in land cover could then be compared to results from carbon accumulation. Results of the spatial assessment were separated into two time periods; 1930 to 1970, the timeframe between the onset of land clearing and the first satellite image, and 1970 to 2010 which provides a more detailed assessment of temporal changes to the study area. The time period 1930 to 1970 was characterized by a rapid removal (peak until the 1960's) of vegetation established at the margins of inland waters; especially *Aniba rosaeodora* (Pau-rosa) for extraction of oils, and *Mezilaurus itauba* and *Cedrela fissilis* (Louro-itaúba and Cedro, respectively) as hardwoods, and the opening of clearings for crops of textile fibers and subsistence products. Intensification of deforestation towards the interior of the forest and following the urban growth of Santarém is reported from the 1970's (Amorim 2000, Cruz et al. 2011). The depletion of vegetation near to the margins of lakes and running waters in this region is also well documented (Amorim 2000, Cruz et al. 2011).

In order to address the spatial dependence of recent OC burial in Jupindá Lake for deforestation, we analyzed the land cover and land use in four buffer areas around the lake and contributing rivers or streams. The first buffer of 100 m represented the riparian forest protected area by the Brazilian laws for fluvial channels with a width of 50 to 200 m. Other buffers were progressively higher, with a width of 500, 1000 and 6000 m from the riverbank and lake margins (Figure 2). In addition, we considered only stretches of rivers and streams 65 km long from Jupindá Lake to analyze its catchment area of more

direct influence. This criteria also avoids the interference of the artificial flooding on the margins of the Curuá-Una hydroelectric dam, which was built in 1977 (Fearnside 2005).

The statistical treatment of variables and OC burial rates, when grouped into different phases, showed assumptions which required parametric analyses, including normal distribution (Kolmogorov-Smirnov, $p > 0.05$) and homogeneity of variance (Bartlett, $p > 0.05$). Thus, we used means and standard errors to represent the distribution of values, and parametric tests were conducted, allowing comparison of different phases. Statistical differences were tested using the one-way ANOVA test followed by Tukey's post test (significance was defined as $p < 0.05$). All the statistical tests used in this work were performed using GraphPad Prism 5.0 software.

3. Results

The analyses of $^{239+240}$Pu showed no detectable activities from the base of the sediment core until the 22-26 cm interval (Figure 3). However, $^{239+240}$Pu was detected in the 18-22 cm interval (0.029 ± 0.002 Bq/kg $^{239+240}$Pu) with the peak concentration (0.047 ± 0.004 Bq/kg $^{239+240}$Pu) at the 16 cm depth, which indicates the 1963 stratospheric fallout peak. Hence material below 22 cm was deposited pre-bomb (that is, prior to the early 1950's). This affixes an upper limit on the average sedimentation rate of near to 3.8 mm year^{-1}. The Pu atom ratio data indicate that the Pu is originating from stratospheric fallout with isotopic ratios ($^{240/239}$Pu) of ~0.18. These results are consistent with the ^{240}Pu/^{239}Pu of 0.180 ± 0.014 discussed by Kelley et al. (1999).

The ^{210}Pb and ^{226}Ra profiles as well as the ^{210}Pb$_{(ex)}$ profile vs cumulative dry mass accumulation reveals a complex depositional environment with sedimentation variations

and disturbances, such as bioturbation and resuspension in the upper ~ 20 cm of the sediment column (Figure 4). A decrease in $^{210}Pb_{ex}$ activity was found below the 20 cm depth interval. The $^{210}Pb_{ex}$ data distribution are as follows: $y = -0.0749x + 7.5$; $R^2 = 0.73$; $n=19$; $p < 0.01$ from the 20 to the 60 cm interval, below the apparent mixed zone. Both estimates of sediment accretion rate during the 120 years from CIC and CRS models were similar, reaching 4.1 and 4.3 mm yr^{-1} respectively, which were slightly higher than the ~ 60 year $^{239+240}Pu$ dates (3.8 mm yr^{-1}). In order to obtain a more reliable estimates of the historical carbon burial rates, the $^{239+240}Pu$ results, from near 1950 to present, were used (3.8 mm $year^{-1}$) and $^{210}Pb_{ex}$ (4.2 mm $year^{-1}$) was used from ~1890 to approximately the 1950s. These rates for each sediment depth were multiplied by the DBD and OC content for each interval of the entire sediment core.

The dry bulk density (DBD), total organic carbon (OC%), total nitrogen (TN%) content as well as the carbon and nitrogen (C/N) molar ratios along with the $\delta^{13}C$ and $\delta^{15}N$ values showed a decreasing shift towards the center of the sediment core (Table 2). The relationship between $\delta^{13}C$ and $\delta^{15}N$ indicated different origins of OC in the sediment core (Figure 5) contributing to the significant relationship between OC burial and the $\delta^{13}C$ (Figure 6). The significantly greater $\delta^{13}C$ peak and lower $\delta^{15}N$ values coupled to higher OC burial rates were observed in the phase between ~1930 to 1970 in Jupindá Lake (one-way ANOVA followed by Tukey's post test, $p<0.05$; Fig. 7). The $\delta^{13}C$ values were greater in the phase ~1930 to 1970 in relation to those previous and after respectively (one-way ANOVA followed by Tukey's post test, $p<0.05$). This peak near 1950 also showed $\delta^{15}N$ values lower and OC burial rates higher than other phases (one-way ANOVA followed by Tukey's post test, $p<0.05$).

241 The OC burial rates indicate an increasing trend from ~ 1930 with a peak during the
242 1940's and 50's (Figure 7). The carbon burial rates increased from ~186 g m^{-2} $year^{-1}$
243 before the 1950s, and up to 298 g m^{-2} $year^{-1}$ between the 1940s and 1950s. Carbon
244 accumulation then decreased to approximately 186 g m^{-2} $year^{-1}$ from 1960 to 1980, after
245 which a gradual decline in carbon burial is noted. In relation to land use/cover in the
246 surrounding fluvial channels and the Jupindá Lake, only the smallest buffer (100 m)
247 showed significant changes during 1930-1970. This time period is when deforestation
248 was nearly 75% higher than in the subsequent time period 1970-2010 (Figure 8a) and
249 when OC burial was greatest (Figure 8b).
250
251 **4. Discussion**
252 Similar estimates of sediment accretion were calculated using different
253 methodologies ($^{239+240}Pu$ and $^{210}Pb_{(ex)}$). These accretion rates along with the dry bulk
254 density revealed an insight into changes in the sediment sources of floodplains, and their
255 relationships with changing land cover and land use in the Amazon Basin. The Jupindá
256 Lake showed substantial changes in the carbon burial rates following deforestation,
257 supporting the connection between flooded areas and their surrounding vegetation. The
258 high peak in carbon accumulation observed around 1950 appears to be associated with a
259 shift in the source of organic material, inferred by changes in carbon and nitrogen
260 contents and the isotopic fractioning toward the middle (from 20 to 40 cm depth interval)
261 of the sediment column. This peak for different organic and inorganic variables in
262 intermediate depths revealed changes not only in the amount but also in the type of
263 material being deposited over time. Previous studies have reported two common origins

for OC in the Amazon forest. Higher $\delta^{15}N$ and more negative $\delta^{13}C$ values could indicate the presence of Santarém soil organic matter (such as that adjacent to the Jupindá Lake), while lower $\delta^{15}N$ and more variable $\delta^{13}C$ values indicate particulate organic carbon (POC) from the terrestrial vegetation in the catchment (Ometto et al. 2006, Zocatelli et al. 2013). Here, a corresponding increase in OC%, TN% and OC burial rates measured, with a peak near 1950, suggesting higher inputs of organic matter into lake. The higher $\delta^{13}C$ signature, coupled with a lower $\delta^{15}N$ indicates a greater influence from the terrestrial Amazonian POC during the same period, around 1950 (Ometto et al., 2006).

When looking for a cause for this change in the source of organic material, we look to the analysis of land use change. Land clearing associated with early occupation from the 1940s in the catchment area of the Jupindá Lake may be a potential cause of the increased carbon burial observed in the lake. Changes in land use and associated deforestation may significantly affect OC burial in mid-high-latitude lakes (Anderson et al. 2013, Dietz et al. 2015). Indeed, our results suggest that land clearing during the 1940's and 50's might be related to increased organic matter deposition in the region's floodplain lakes. During this period, intense wood extraction and expansion of agricultural settlements occurred (Amorim 2000, Cruz et al. 2011). One important consequence of deforestation in the watershed is the silting up of lakes (Enea et al. 2012), including those at humid low-latitude areas (Cohen et al. 2005, Bakoariniaina et al. 2006). However, the lake is in a region relatively well protected, and therefore there is no other explanation other than deforestation in the margins to have caused the peak in OC burial near the 1950s. The riparian forest systems are generally effective in reducing the sediment transport by surface runoff, with the removal of this vegetation increasing the erosion processes,

especially in the Amazon Basin as a result of intense rainfall (Neill et al. 2013a). The peak of the significantly greater $\delta^{13}C$ and lower $\delta^{15}N$ values coupled to higher OC burial rates were observed in the phase between ~1930 to 1970 in Jupindá Lake (one-way ANOVA followed by Tukey's post test, $p<0.05$; Fig. 7). The $\delta^{13}C$ values were greater in the ~1930 to 1970 phase as related to those previous and after respectively (one-way ANOVA followed by Tukey's post test, $p<0.05$). This peak between ~1930 to 1970 also showed delta $\delta^{15}N$ values lower and OC burial rates higher than other phases (one-way ANOVA followed by Tukey's post test, $p<0.05$).

We also found a spatial dependence of the carbon accumulation in Lake Jupindá, as the much lower OC burial was coupled to higher deforestation rates in those larger buffers around its margins and main fluvial channels (500, 1000 and 6000 m) in the period after 1970s (between the 1970s to 2010) than that before (~1930 to 1970). This confirms previous evidence that the recent deforestation process in the region commenced in the riparian zone (Amorim 2000, Cruz et al. 2011), and not in the interior of the forest. The enhanced OC burial in lacustrine sediments before ~1970 was related to higher deforestation rates only in the riparian vegetation zone (100 m buffers), suggesting a higher influence of deforestation with decreasing distance to water courses. Therefore, the soil carbon enrichment to the aquatic sediments during the peaks of riparian deforestation may cause intense but temporary carbon burial events in the Amazon floodplain, representing potentially only a significant part of the total loss of terrestrial organic matter. In addition, the continued removal of vegetation from the interior of the forest might not be directly related to increases of OC burial, even temporarily, in depositional aquatic ecosystems.

5. Conclusion

Palaeolimnological techniques were used with a historical spatial analysis of deforestation to interpret changes in sediment characteristics during the past century. The Pu dating method closely approximates measurements from the ^{210}Pb chronologies and hence offers a technique to determine sedimentation rates and carbon accumulation in Amazon sediments. An increase in OC burial, up to 298 OC g m^{-2} $year^{-1}$, coincides with changes in the $\delta^{13}C$ and $\delta^{15}N$ signatures, likely influenced by the heavy deforestation in riparian systems of this region during the 1940s and 1950s. It is suggested that the net increase in carbon burial towards the center of the sediment core , which represents the highest carbon burial rates during the 1950s, is a result of a change in source of organic matter deposition. However, any increase of OC burial rates attributed to deforestation might be lower than the loss of terrestrial biomass in the standing crop or soils. The differing carbon burial rates along the sediment core therefore identify the potential complexity of the Amazon floodplain lakes, directly related to the development within the Basin. This work supports the urgent need for management practices based on the conservation of riparian forests, demonstrating the spatial dependence of carbon burial capacity of the Amazon floodplain lakes with respect to advances in deforestation in the Basin.

Acknowledgements

LMS is supported by an APA and IPRS scholarships. HM received a research grant from the Brazilian Research Council (CNPq – “Programa Universal”) and the Research

Support Foundation of the State of Rio de Janeiro (FAPERJ – "Programa Jovem Cientista do Nosso Estado"). CJS is supported by the Australian Research Council (DE160100443).

CAPTIONS TO FIGURES

Figure 1. Jupindá Lake where the sediment core was extracted, near the Amazon River and the city of Santarém, Brazil. This floodplain lake has a diameter of approximately 3 km.

Figure 2. Different buffer sizes (100 m, 500 m, 1 km and 6 km) along the stretch of the Curuá-Una River from Jupindá Lake (red) to the hydroelectric dam upstream (yellow).

Figure 3. $^{239+240}$Pu profile, indicating ~ 1950 when these radionuclides were first introduced into the atmosphere.

Figure 4. Lead-210 (black circles) and ^{226}Ra (white circles) profiles against depth. Grey squares represent the ^{210}Pb(ex) profile vs cumulative dry mass.

Figure 5. δ^{13}C vs δ^{15}N. The Amazon River POM and Santarem soil organic matter values, adjacent to the study area, are taken from Zocatelli et al (2013).

Figure 6. Carbon burial as a function of δ^{13}C and δ^{15}N.

Figure 7. δ^{13}C, δ^{15}N and carbon burial rate values in relation to depth (cm). Panels below each vertical profile represent respective data grouped by the three general phases >1930, 1930-1970 and 1970-2010. Filled square symbols represent means of a given variable in each sediment layer, and the vertical bars show the mean with the standard

deviation of the respective phase. Equal letters in each panel represent non-significant differences ($p > 0.05$, one-way ANOVA followed by Tukey's post test).

Figure 8. Percentage of modified areas in relation to the different buffers (Panel A). Carbon burial (black dots) and changes in the riparian vegetation (two grey bars represent the two general phases) as related to time (Panel B).

CAPTION TO TABLES

Table 1. Satellite acquisition data from United States Geological Survey (USGS) and the Curuá-Una River quota from Brazilian Water Agency (ANA).

Table 2. Depth profiles of dry bulk density (DBD), total organic carbon (OC%), total nitrogen (TN%) carbon and nitrogen (C/N) molar ratios, $\delta^{13}C$ and $\delta^{15}N$.

Table 1.

Month/Year	*Landsat Data*	*Curuá-Una River Quote*
Aug/1975	2	5.3
Oct/1985	5	3.7
June/1995	5	6
June/2008	5	*No data*

Table 2.

Depth (cm)	DBD (g cm^{-3})	$\delta^{15}N$	$\delta^{13}C$	C (%)	N (%)	C/N
0-2	1.0	8.9	-29.2	3.8	0.3	17.2
2-4	0.9	11.7	-29.0	3.8	0.3	18.7
4-6	1.0	10.4	-28.8	4.0	0.3	19.2
6-8	1.1	9.3	-28.7	4.3	0.3	20.2
8-10	1.0	9.4	-28.7	4.1	0.3	19.8
10-12	1.1	7.9	-28.6	4.6	0.3	21.2
12-14	1.1	8.2	-28.7	4.3	0.3	19.9
14-16	1.1	7.8	-28.6	4.3	0.3	20.9
16-18	1.0	8.7	-28.5	4.4	0.3	21.2
18-20	1.1	7.5	-28.4	4.4	0.3	19.8
20-22	1.0	6.5	-28.2	5.4	0.3	21.2
22-24	1.0	6.0	-27.8	5.3	0.3	21.5
24-26	1.0	5.2	-27.4	7.3	0.4	25.4
26-28	1.1	6.1	-27.6	6.0	0.3	23.8
28-30	1.0	5.0	-27.3	6.0	0.4	22.7
30-32	1.0	5.4	-28.0	6.1	0.3	27.0
32-34	1.3	6.6	-28.5	4.4	0.2	27.5
34-36	1.6	8.9	-29.0	2.2	0.1	23.1
36-38	1.4	11.4	-29.4	2.9	0.1	30.4
38-40	1.4	10.4	-29.5	3.3	0.1	30.5
40-42	1.5	11.4	-29.3	2.4	0.1	23.8
42-44	1.6	12.2	-29.4	1.3	0.1	15.6
44-46	1.8	8.2	-29.6	1.2	0.1	14.3
46-48	1.5	8.8	-29.8	2.2	0.1	21.6
48-50	0.9	10.4	-29.7	2.9	0.2	25.6
50-52	0.9	10.2	-29.7	2.6	0.1	27.2
52-54	0.9	7.1	-29.7	3.9	0.2	28.6
54-56	0.9	9.2	-29.9	3.6	0.2	27.8
56-58	0.9	6.6	-30.1	4.3	0.2	30.1
58-60	0.9	5.0	-30.1	3.5	0.2	23.1
Average	**1.11**	**8.34**	**-28.9**	**4.0**	**0.2**	**23.0**
Stand Dev	**0.24**	**2.1**	**0.8**	**1.9**	**0.1**	**4.2**

399 **References**
400
401 Aalto, R., L. Maurice-Bourgoin, T. Dunne, D. R. Montgomery, C. A. Nittrouer, and J. L.
402 Guyot. 2003. Episodic sediment accumulation on Amazonian flood plains
403 influenced by El Niño/Southern Oscillation. Nature **425**:493-497.
404 Abril, G., J. M. Martinez, L. F. Artigas, P. Moreira-Turcq, M. F. Benedetti, L. Vidal, T.
405 Meziane, J. H. Kim, M. C. Bernardes, N. Savoye, J. Deborde, E. L. Souza, P.
406 Albéric, M. F. Landim De Souza, and F. Roland. 2014. Amazon River carbon
407 dioxide outgassing fuelled by wetlands. Nature **505**:395-398.
408 Amorim, A. T. d. S. 2000. Santarém: uma síntese histórica, Canoas, Ulbra, Santarem,
409 Brazil
410 Anderson, N. J., R. D. Dietz, and D. R. Engstrom. 2013. Land-use change, not climate,
411 controls organic carbon burial in lakes. Proceedings. Biological sciences / The
412 Royal Society **280**:20131278.
413 Appleby, P. G., and F. Oldfield. 1992. Application of lead-210 to sedimentation studies.
414 Pages 731-783 *in* M. Ivanovich and S. Harmon, editors. Uranium Series
415 Disequilibrium: Application to Earth, Marine and Environmental Science. Oxford
416 Science Publications.
417 Bakoariniaina, L. N., T. Kusky, and T. Raharimahefa. 2006. Disappearing Lake Alaotra:
418 Monitoring catastrophic erosion, waterway silting, and land degradation hazards
419 in Madagascar using Landsat imagery. Journal of African Earth Sciences **44**:241-
420 252.
421 Brodie, C. R., J. S. L. Casford, J. M. Lloyd, M. J. Leng, T. Heaton, C. P. Kendrick, and
422 Z. Yongqiang. 2011. Evidence for bias in C/N, δ13C and δ15N values of bulk
423 organic matter, and on environmental interpretation, from a lake sedimentary

sequence by pre-analysis acid treatment methods. Quaternary Science Reviews **30**:3076-3087.

Cohen, A. S., M. R. Palacios-Fest, J. McGill, P. W. Swarzenski, D. Verschuren, R. Sinyinza, T. Songori, B. Kakagozo, M. Syampila, C. M. O'Reilly, and S. R. Alin. 2005. Paleolimnological investigations of anthropogenic environmental change in Lake Tanganyika: I. An introduction to the project. Journal of Paleolimnology **34**:1-18.

Cruz, H., P. Sablayrolles, M. Kanashiro, and M. S. Amaral, P. 2011. Relação empresa/ comunidade no manejo florestal comunitário e familiar: Uma contribuição do Projeto Floresta em pé.

Diaz, R. J., and R. Rosenberg. 2008. Spreading dead zones and consequences for marine ecosystems. Science **321**:926-929.

Dietz, R. D., D. R. Engstrom, and N. J. Anderson. 2015. Patterns and drivers of change in organic carbon burial across a diverse landscape: Insights from 116 Minnesota lakes. Global Biogeochemical Cycles **29**:708-727.

Dong, X., N. J. Anderson, X. Yang, X. chen, and J. Shen. 2012. Carbon burial by shallow lakes on the Yangtze floodplain and its relevance to regional carbon sequestration. Global Change Biology **18**:2205-2217.

Downing, J. P., M. Meybeck, J. C. Orr, R. R. Twilley, and H. W. Scharpenseel. 1993. Land and water interface zones. Water, Air, & Soil Pollution **70**:123-137.

Enea, A., G. Romanescu, and C. Stoleriu. 2012 Quantitative considerations concerning the source-areas for the silting of the red lake (Romania) lacustrine basin.

. Romania.

447 Fearnside, P. M. 2005. Do hydroelectric dams mitigate global warming? The case of
448 Brazil's Curuá-Una Dam. Mitigation and Adaptation Strategies for Global Change
449 **10**:675-691.
450 Gordon, S. I. 1980. Utilizing LANDSAT imagery to monitor land-use change: A case
451 study in ohio. Remote Sensing of Environment **9**:189-196.
452 Goulding, M. 1993. Flooded forests of the Amazon. Scientific American **268**:114-
453 120+115.
454 Hoffmann, T., M. Schlummer, B. Notebaert, G. Verstraeten, and O. Korup. 2013. Carbon
455 burial in soil sediments from Holocene agricultural erosion, Central Europe.
456 Global Biogeochemical Cycles **27**:828-835.
457 INPE. 2016. Program for the Estimation of Amazon Deforestation. Accessed 20
458 November 2016, http://www.obt.inpe.br/prodes/prodes_1988_2015n.htm.
459 Ivanovich, M., and S. Harmon. 1992. Uranium Series Disequilibrium - Applications to
460 Earth, Marine and Environmental Sciences. second edition edition. Oxford
461 Science Publications.
462 Junk, W. J. 2013. Current state of knowledge regarding South America wetlands and
463 their future under global climate change. Aquatic Sciences **75**:113-131.
464 Ketterer, M. E., K. M. Hafer, V. J. Jones, and P. G. Appleby. 2004. Rapid dating of
465 recent sediments in Loch Ness: Inductively coupled plasma mass spectrometric
466 measurements of global fallout plutonium. Science of the Total Environment
467 **322**:221-229.
468 LigockI, L. P. 2003. Comportamento geotécnico da barragem de Curuá-Una, Pará. Rio de
469 Janeiro.

Lucas, C. M., J. Schöngart, P. Sheikh, F. Wittmann, M. T. F. Piedade, and D. G. McGrath. 2014. Effects of land-use and hydroperiod on aboveground biomass and productivity of secondary Amazonian floodplain forests. Forest Ecology and Management **319**:116-127.

Marotta, H., L. Bento, F. A. De Esteves, and A. Enrich-Prast. 2009. Whole ecosystem evidence of eutrophication enhancement by wetland dredging in a shallow Tropical Lake. Estuaries and Coasts **32**:654-660.

Marotta, H., C. M. Duarte, F. Meirelles-Pereira, L. Bento, F. A. Esteves, and A. Enrich-Prast. 2010. Long-term CO2 variability in two shallow tropical lakes experiencing episodic eutrophication and acidification events. Ecosystems **13**:382-392.

Marotta, H., L. Pinho, C. Gudasz, D. Bastviken, L. J. Tranvik, and A. Enrich-Prast. 2014. Greenhouse gas production in low-latitude lake sediments responds strongly to warming. Nature Climate Change **4**:467-470.

Melack, J. M., L. L. Hess, M. Gastil, B. R. Forsberg, S. K. Hamilton, I. B. T. Lima, and E. M. L. M. Novo. 2004. Regionalization of methane emissions in the Amazon Basin with microwave remote sensing. Global Change Biology **10**:530-544.

Munyati, C. 2000. Wetland change detection on the Kafue Flats, Zambia, by classification of a multitemporal remote sensing image dataset. International Journal of Remote Sensing **21**:1787-1806.

Naidu, A. S., L. W. Cooper, B. P. Finney, R. W. Macdonald, C. Alexander, and I. P. Semiletov. 2000. Organic carbon isotope ratio (δ13C) of Arctic Amerasian Continental shelf sediments. International Journal of Earth Sciences **89**:522-532.

492 Neill, C., M. T. Coe, S. H. Riskin, A. V. Krusche, H. Elsenbeer, M. N. Macedo, R.
493 McHorney, P. Lefebvre, E. A. Davidson, R. Scheffler, A. M. e Silva Figueira, S.
494 Porder, and L. A. Deegan. 2013a. Watershed responses to Amazon soya bean
495 cropland expansion and intensification. Philosophical Transactions of the Royal
496 Society B: Biological Sciences **368**.
497 Neill, C., M. T. Coe, S. H. Riskin, A. V. Krusche, H. Elsenbeer, M. N. Macedo, R.
498 McHorney, P. Lefebvre, E. A. Davidson, R. Scheffler, A. M. Figueira, S. Porder,
499 and L. A. Deegan. 2013b. Watershed responses to Amazon soya bean cropland
500 expansion and intensification. Philosophical transactions of the Royal Society of
501 London. Series B, Biological sciences **368**:20120425.
502 Neue, H. U., J. L. Gaunt, Z. P. Wang, P. Becker-Heidmann, and C. Quijano. 1997.
503 Carbon in tropical wetlands. Geoderma **79**:163-185.
504 Ometto, J. P. H. B., J. R. Ehleringer, T. F. Domingues, J. A. Berry, F. Y. Ishida, E.
505 Mazzi, N. Higuchi, L. B. Flanagan, G. B. Nardoto, and L. A. Martinelli. 2006.
506 The stable carbon and nitrogen isotopic composition of vegetation in tropical
507 forests of the Amazon Basin, Brazil. Biogeochemistry **79**:251-274.
508 Peixoto, R. B., H. Marotta, D. Bastviken, and A. Enrich-Prast. 2016. Floating Aquatic
509 Macrophytes Can Substantially Offset Open Water CO<inf>2</inf> Emissions
510 from Tropical Floodplain Lake Ecosystems. Ecosystems **19**:724-736.
511 Sanders, C. J., B. D. Eyre, I. R. Santos, W. MacHado, W. Luiz-Silva, J. M. Smoak, J. L.
512 Breithaupt, M. E. Ketterer, L. Sanders, H. Marotta, and E. Silva-Filho. 2014.
513 Elevated rates of organic carbon, nitrogen, and phosphorus accumulation in a
514 highly impacted mangrove wetland. Geophysical Research Letters **41**:2475-2480.

Sanders, C. J., I. R. Santos, D. T. Maher, J. L. Breithaupt, J. M. Smoak, M. Ketterer, M. Call, L. Sanders, and B. D. Eyre. 2016. Examining 239+240Pu, 210Pb and historical events to determine carbon, nitrogen and phosphorus burial in mangrove sediments of Moreton Bay, Australia. Journal of Environmental Radioactivity **151**:623-629.

Sanders, L. M., K. H. Taffs, D. J. Stokes, C. J. Sanders, J. M. Smoak, A. Enrich-Prast, P. Macklin, I. R. Santos, and H. Marotta. 2017. Carbon accumulation in Amazonian floodplain lakes: A significant component of Amazon budgets? Limnology & Oceanography Letters:29-35.

Skole, D., and C. Tucker. 1993. Tropical deforestation and habitat fragmentation in the amazon: Satellite data from 1978 to 1988. Science **260**:1905-1910.

Smith, L. K., J. M. Melack, and D. E. Hammond. 2002. Carbon, nitrogen, and phosphorus content and 210Pb-derived burial rates in sediments of an Amazon floodplain lake. Amazoniana **17**:413-436.

Stanley, E. H., S. M. Powers, N. R. Lottig, I. Buffam, and J. T. Crawford. 2012. Contemporary changes in dissolved organic carbon (DOC) in human-dominated rivers: Is there a role for DOC management? Freshwater Biology **57**:26-42.

Zocatelli, R., P. Moreira-Turcq, M. Bernardes, B. Turcq, R. C. Cordeiro, S. Gogo, J. R. Disnar, and M. Boussafir. 2013. Sedimentary evidence of soil organic matter input to the curuai amazonian floodplain. Organic Geochemistry **63**:40-47.

Figure 1.

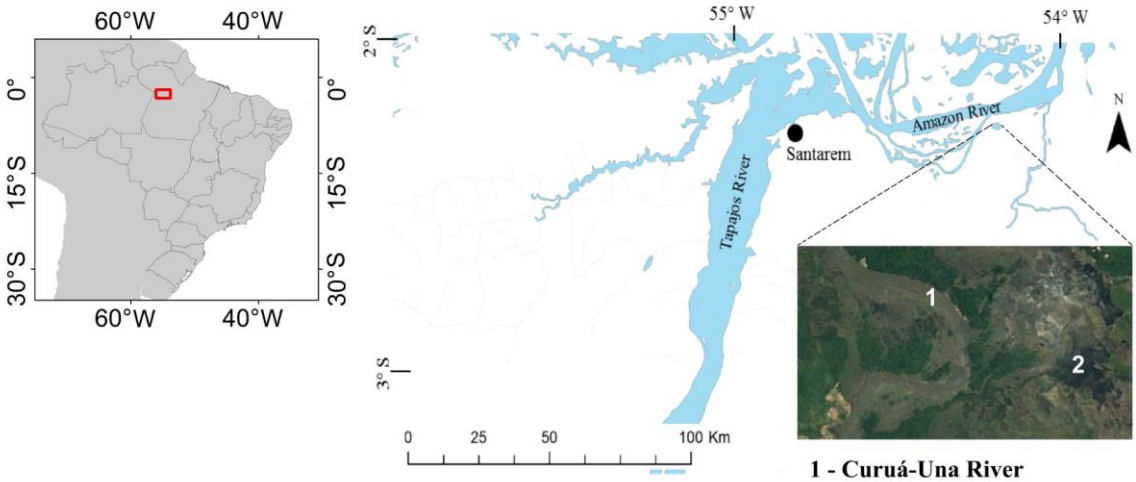
60°W
40°W
0°
15°S
30°S
2° S
3° S
55° W
54° W
N
Amazon River
Santarem
Tapajos River
0
25
50
100 Km
1
2
1 - Curuá-Una River
2 - Floodplain Lake Jupindá

Figure 2.

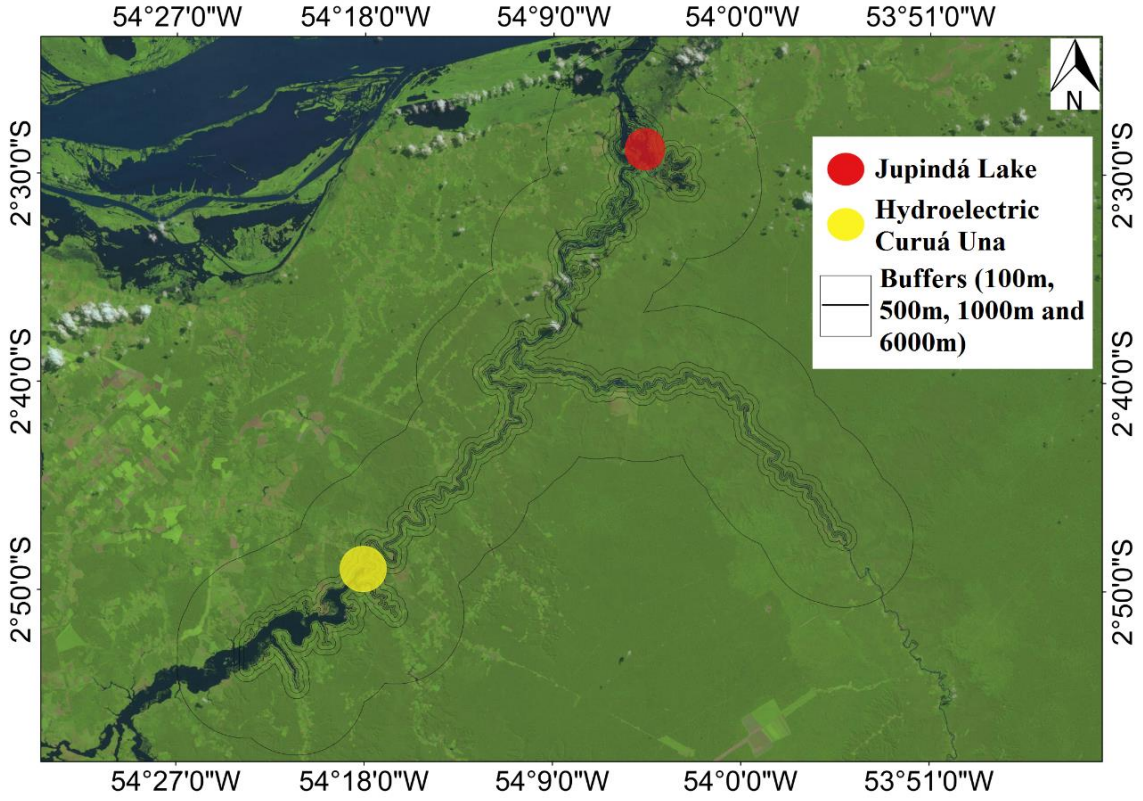
54°27'0"W
54°18'0"W
54°9'0"W
54°0'0"W
53°51'0"W
2°30'0"S
2°40'0"S
2°50'0"S
N
Jupindá Lake
Hydroelectric Curuá Una
Buffers (100m, 500m, 1000m and 6000m)

Figure 3.

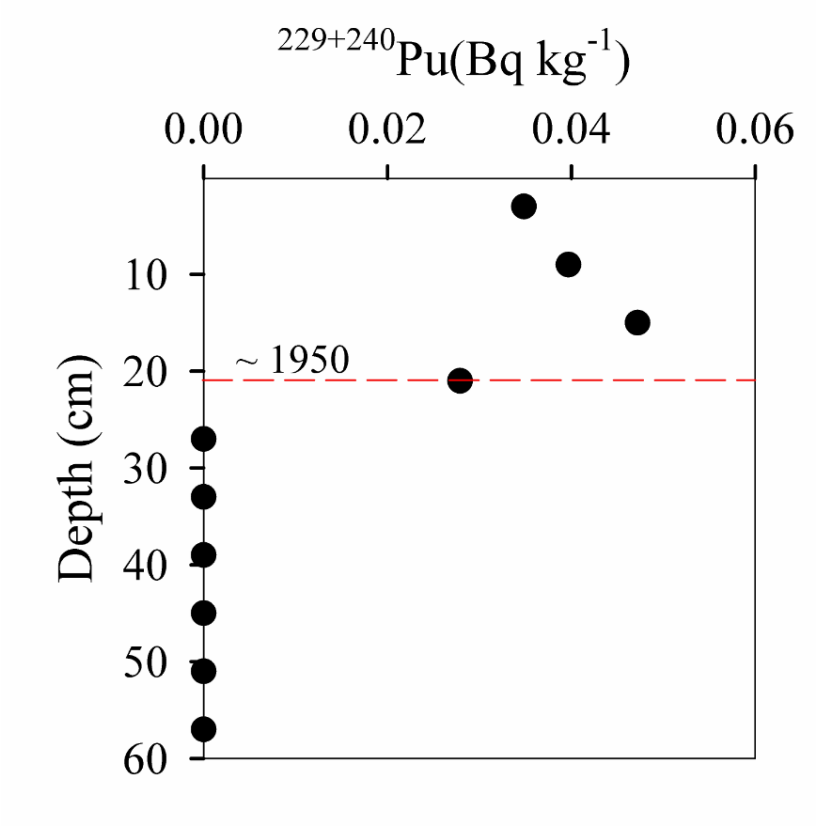

Figure 4.

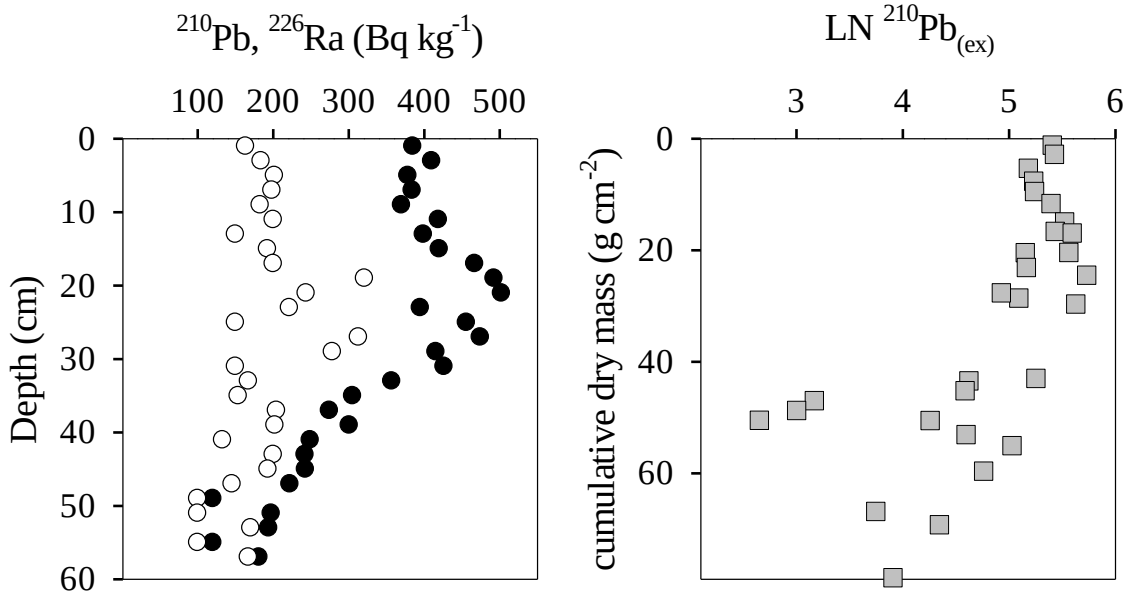
^{210}Pb, ^{226}Ra (Bq kg^{-1})
100 200 300 400 500
Depth (cm)
0 10 20 30 40 50 60
LN ^{210}Pb$_{(ex)}$
3 4 5 6
cumulative dry mass (g cm^{-2})
0 20 40 60

Figure 5.

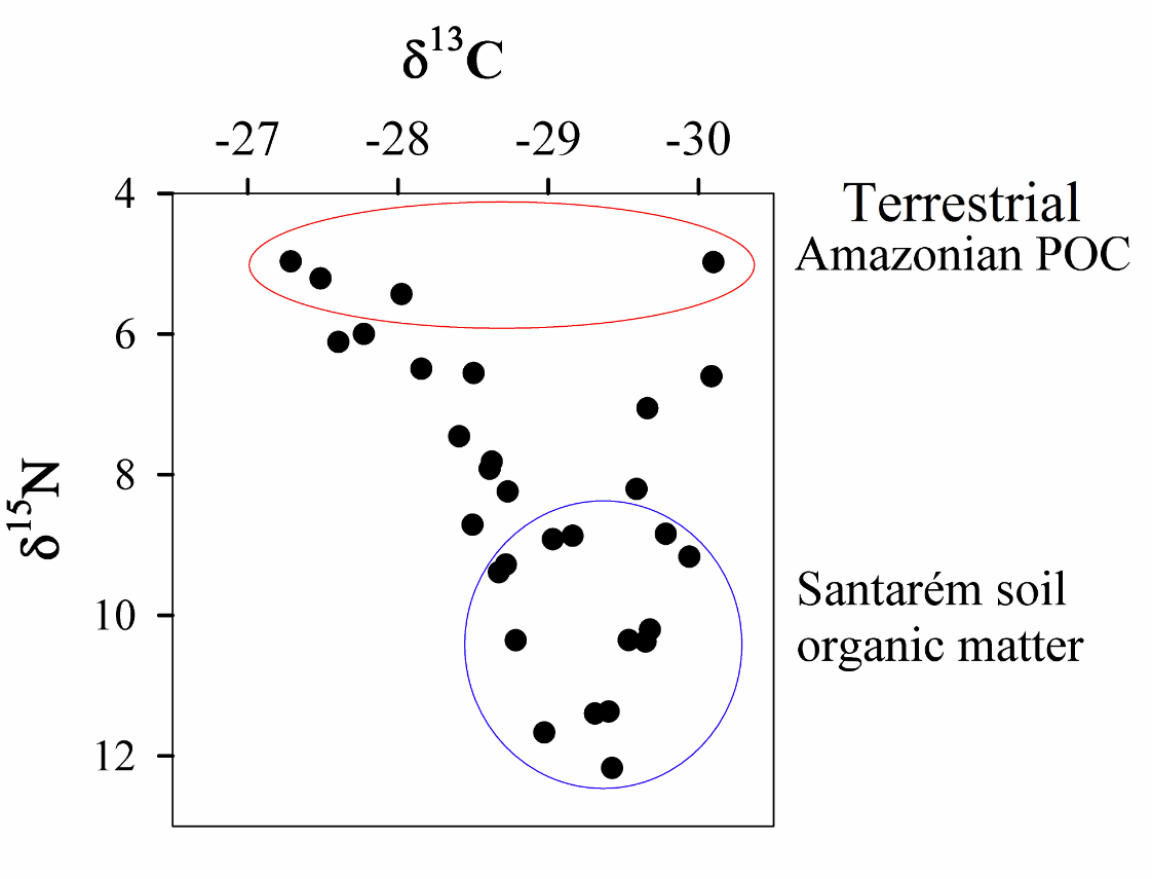
δ13C
-27
-28
-29
-30
4
6
8
10
12
δ15N
Terrestrial
Amazonian POC
Santarém soil
organic matter

Figure 6.

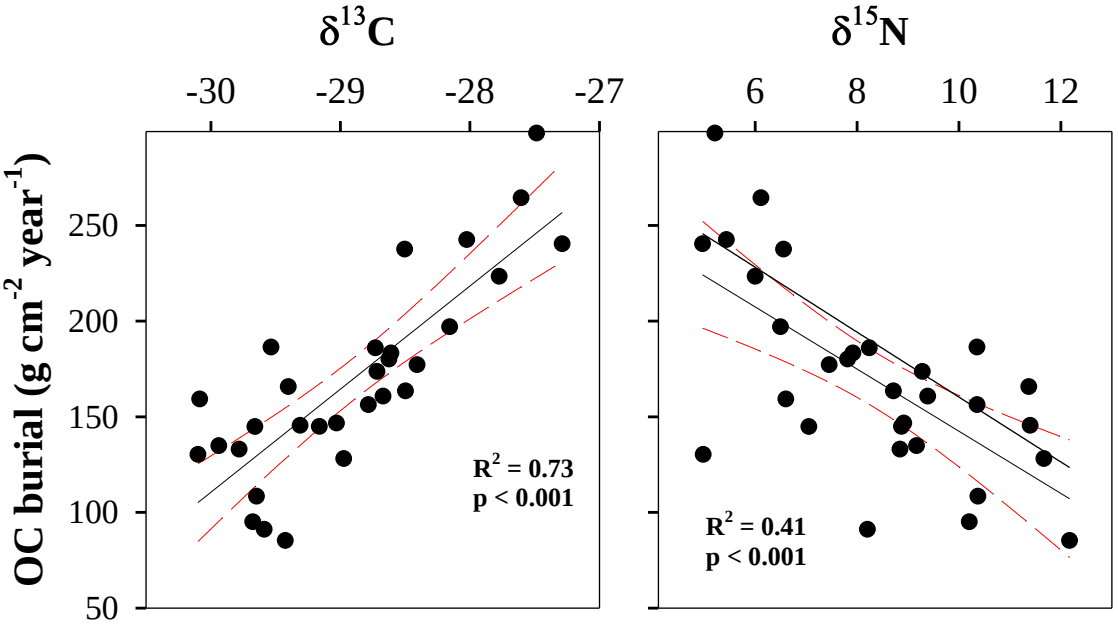
δ13C
δ15N
-30
-29
-28
-27
6
8
10
12
OC burial (g cm-2 year-1)
250
200
150
100
50
R2 = 0.73
p < 0.001
R2 = 0.41
p < 0.001

Figure 7.

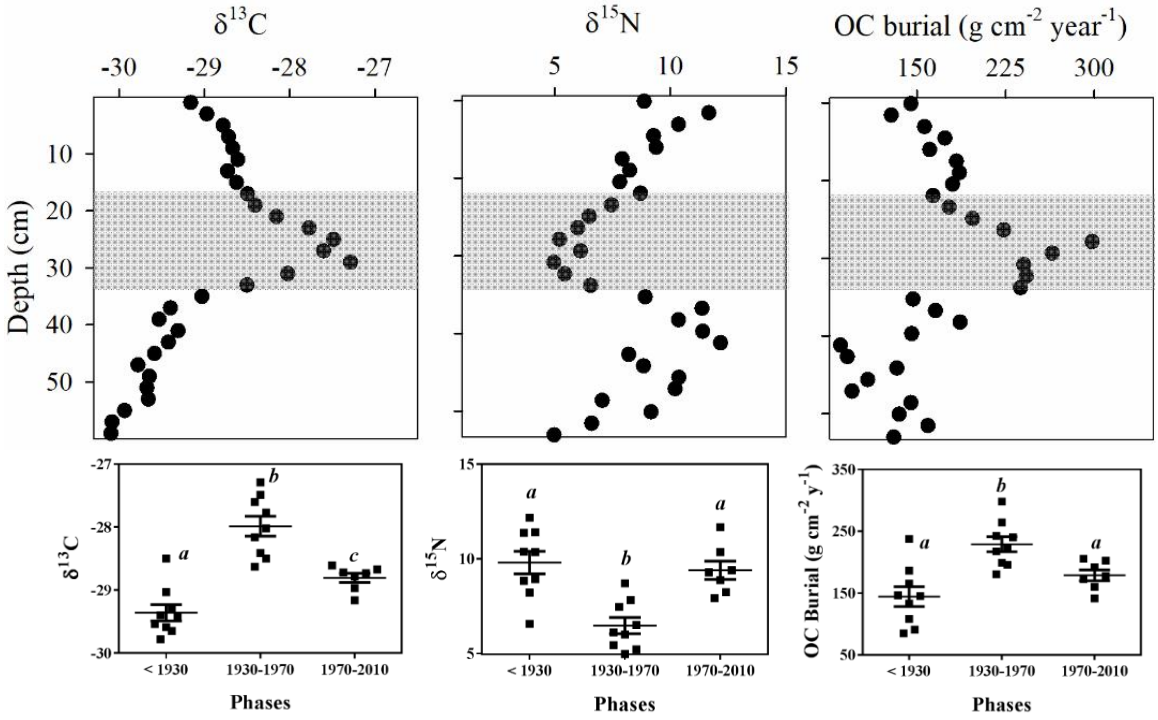
δ13C
δ15N
OC burial (g cm-2 year-1)
Depth (cm)
-30
-29
-28
-27
5
10
15
150
225
300
10
20
30
40
50
δ13C
δ15N
OC Burial (g cm-2 y-1)
a
b
c
< 1930
1930-1970
1970-2010
Phases

732 **Figure 8.**

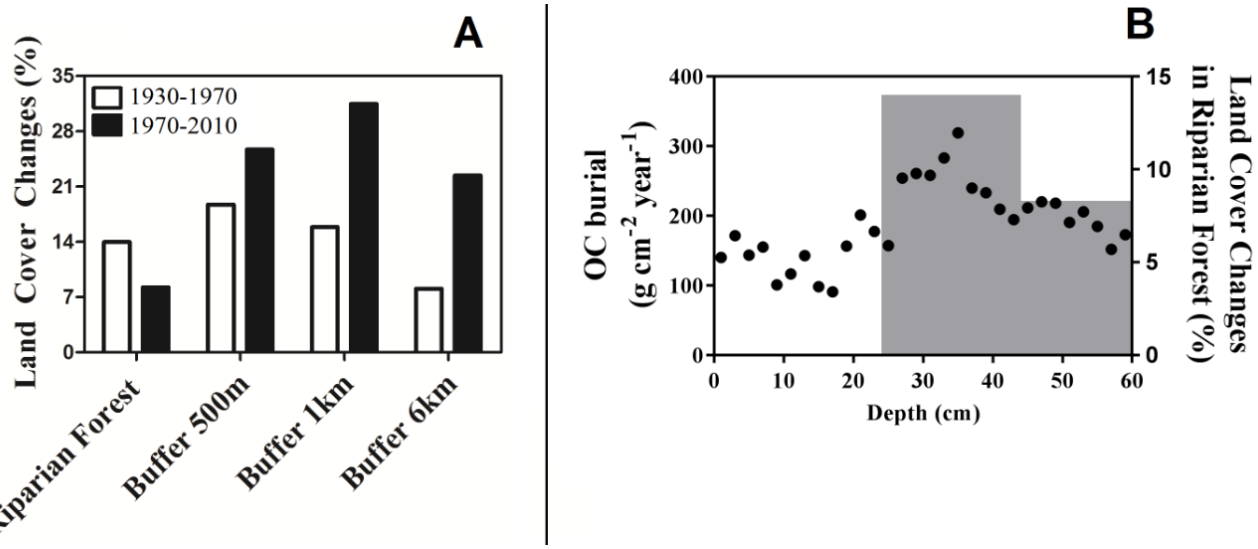

733